ELSEVIER

Surface and Coatings Technology 92 (1997) 206–211

SURFACE & COATINGS TECHNOLOGY

Ion nitriding of equiatomic TiNi shape memory alloys II. Corrosion properties and wear characteristics

S.K. Wu *, C.L. Chu, H.C. Lin [1]

Institute of Materials Science and Engineering, National Taiwan University, Taipei 106, Taiwan

Received 2 January 1997; accepted 10 March 1997

Abstract

The corrosion properties and wear characteristics of $Ti_{50}Ni_{50}$ and $Ti_{50}Ni_{40}Cu_{10}$ shape memory alloys with and without ion nitriding were investigated by acid immersion test, electrochemical potentiodynamic measurement and sliding wear test. Experimental results indicate that the non-ion-nitrided TiNi specimens are easily attacked by the HCl and H_2SO_4 solutions. However, their corrosion properties in these solutions can be markedly improved by ion nitriding. The improved corrosion resistance is attributed to the TiN compound formed in the outermost part of ion-nitrided layers. In addition, the ion-nitrided TiNi specimens, being hardened by the TiN/Ti_2Ni compound layers, can exhibit excellent wear resistance and a low friction coefficient. © 1997 Published by Elsevier Science S.A.

Keywords: Ion nitriding; Shape memory alloys; TiNi alloys

1. Introduction

Among the many shape memory alloys (SMAs), TiNi alloys are the most popular because they possess superior properties in shape memory effect (SME) [1] and pseudoelasticity (PE) [2,3]. Most of their industrial applications may not involve any corrosion problems. Nevertheless, for applications in orthopedic surgery and medical implantation, or for structural components in corrosive environments, corrosion could be a very critical problem. Several investigations [4–8] have been performed on the corrosion resistance of TiNi alloys. These studies concluded that the TiNi alloys can exhibit fairly good corrosion resistance due to the formation of a thin passive film. However, this passive film can be locally destroyed in some specific environments leading to the occurrence of corrosion. Hence, the improvement of the corrosion resistance of TiNi alloys is necessary to extend their applications in corrosive environments.

Nitriding techniques are often used to increase the surface hardness and to improve the fatigue and wear resistance of metals and alloys [9]. In Part I of this study [10], we found that the surface hardness of $Ti_{50}Ni_{50}$ and $Ti_{50}Ni_{40}Cu_{10}$ alloys can be significantly improved by ion nitriding. This improvement in surface hardness is attributed to the formation of TiN and Ti_2Ni in the surface layers. Nitriding techniques have also been used to improve the corrosion resistance of titanium and titanium alloys [11–17]. However, to the best of our knowledge, there have been few investigations on the corrosion characteristics of ion-nitrided TiNi alloys. In the present study, the corrosion properties of ion-nitrided $Ti_{50}Ni_{50}$ and $Ti_{50}Ni_{40}Cu_{10}$ alloys in hydrochloric acid and sulfuric acid aqueous solutions are investigated. The effects of ion-nitriding parameters on their corrosion resistance are discussed. Meanwhile, the preliminary results of wear characteristics of ion-nitrided $Ti_{50}Ni_{50}$ and $Ti_{50}Ni_{40}Cu_{10}$ alloys are also reported.

2. Experimental procedures

2.1. Specimen preparation

A conventional tungsten arc melting technique was employed to prepare the $Ti_{50}Ni_{50}$ and $Ti_{50}Ni_{40}Cu_{10}$ (in at.%) alloys. Titanium (purity 99.7%), nickel (purity 99.9%) and copper (purity 99.9%), totaling 200 g, were

* Corresponding author.

[1]Present address: Department of Materials Science, Feng Chia University, Taichung 400, Taiwan.

0257-8972/97/$17.00 © 1997 Published by Elsevier Science S.A. All rights reserved.

PII S0257-8972(97)00101-1

melted and remelted at least six times in an argon atmosphere.

Ion nitriding was carried out in an NDK furnace model JIN-6SS-C-SV. The specimen's support and holder were made of titanium to reduce contamination of the specimen surface during the sputtering process. After nitriding, the specimens were cooled in vacuum. The cooling rate was approximately 20 °C s^{-1} at the initial stage, but this rate was slow towards the end of the cooling period. The details of the specimen preparation and the ion-nitriding processes have been described in Part I of this study [10].

2.2. Immersion test

All immersion experiments were conducted at 25 °C in 1 M HCl or 1 M H_2SO_4 solutions for 5–14 days. Following this, specimens were removed and cleaned in ethyl alcohol using ultrasonic equipment. Thereafter, they were weighed and recorded and the corrosion rates were calculated.

2.3. Electrochemical potentiodynamic measurement

Specimens with and without ion nitriding were examined by electrochemical potentiodynamic measurements. The experimental set-up, shown in Fig. 1, included a three-electrode system, a Nichia model NP G1001ED potentio-galvanostat, a potential scanner ES-511A and a personal computer. Scans were initiated by lowering the corrosion potential of the specimen to a pre-set value of −1.0 V (versus the saturated Ag/AgCl electrode), and then scanned to +1.0 V (versus the saturated Ag/AgCl electrode) at a rate of 1 mV s^{-1}; following this, a scan was run from +1.0 V to −1.0 V at the same rate to complete a cycle. The experiment was conducted in a 0.5 M HCl solution at room temperature under static and atmospheric conditions. A platinum sheet was used as a counter electrode and oxygen was removed from the electrolyte by purging with purified nitrogen. In order to minimize the internal resistance drop in the solution, the reference electrode was positioned as closely as possible to the working electrode.

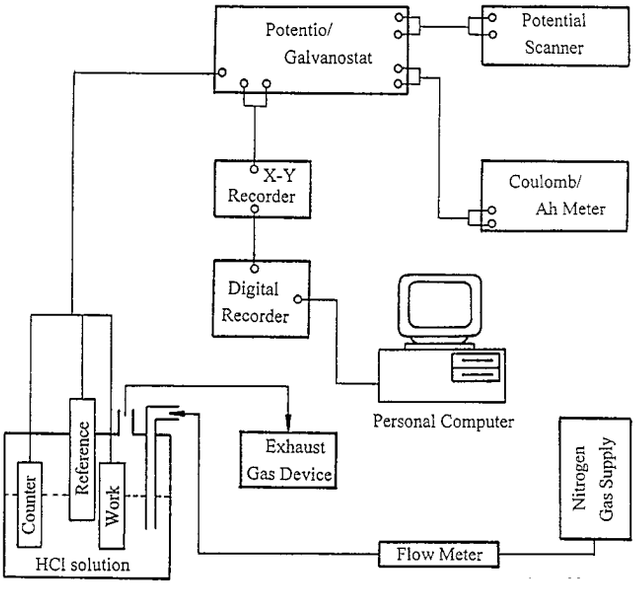

Fig. 1. Schematic diagram of electrochemical potentiodynamic instruments.

2.4. Surface analysis and cross-section microanalysis

After the experiment in Section 2.2, the surface of the specimens were investigated using a Philips 515 scanning electron microscope (SEM) with an energy-dispersive X-ray (EDX) analysis facility. The cross-sections of these specimens were examined by a JEOL JXA-8600SX electron probe microanalyzer (EPMA). X-ray diffraction (XRD) tests were carried out using a Philips PW1710 X-ray diffractor which provided Cu Kα radiation. The power was 40 kV × 30 mA and the 2θ scanning rate was 3° min^{-1}.

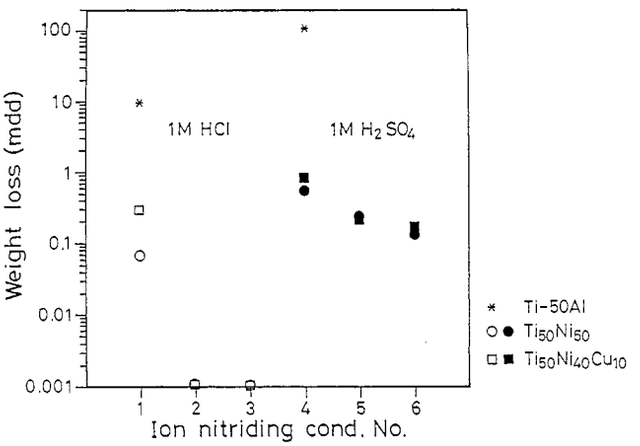

Fig. 2. Immersion test results in 1 M HCl or H_2SO_4 solutions. The ion-nitriding conditions are listed in Table 1.

Table 1
Ion-nitriding conditions of Figs. 2 and 7(b)

Number	Ion-nitriding conditions	Remark
1	None	Fig. 2
2	700 °C for 12 h, 10 torr, $[N_2]/[H_2]=1$	Fig. 2
3	800 °C for 12 h, 6 torr, $[N_2]/[H_2]=4$	Fig. 2
4	None	Fig. 2
5	700 °C for 4 h, 8 torr, $[N_2]/[H_2]=4$	Fig. 2
6	900 °C for 4 h, 6 torr, $[N_2]/[H_2]=1$	Fig. 2
7	900 °C for 12 h, 8 torr, $[N_2]/[H_2]=10$	Fig. 7(b)

2.5. Wear test

The wear tests were performed using a TE-53-type uni-directional sliding wear machine made by Plint and Partners Co., UK. The JIS SKS-95 steel, with hardness 700 HV, was used as the against-wear material. The tests were conducted at a constant wear load of 10 N and a sliding speed of 62.8 cm s^{-1}. The surface morphologies of the worn specimens were observed using a Philips 515 SEM. The average wear rate and friction coefficient were automatically calculated by a digital computer during the sliding wear process.

3. Results and discussion

3.1. Corrosion characteristics of ion-nitrided $Ti_{50}Ni_{50}$ and $Ti_{50}Ni_{40}Cu_{10}$ alloys

Corrosion data from the immersion tests are plotted in Fig. 2 in terms of weight loss versus ion-nitriding conditions. The data from the non-ion-nitrided Ti–50Al specimens (conditions 1 and 4) are also plotted for comparison. In Fig. 2, the symbols in the left half of the diagram are the data points for samples exposed to a 1 M HCl solution; those in the right half are for samples exposed to 1 M H_2SO_4. The ion-nitriding conditions of specimens used in Fig. 2 are listed in Table 1. From Fig. 2, one can see that both $Ti_{50}Ni_{50}$ and $Ti_{50}Ni_{40}Cu_{10}$ alloys are more corrosion resistant than the Ti–50Al specimen and the corrosion rate in H_2SO_4 solution is higher than that in HCl solution. At the same time, the ion-nitrided specimens have better corrosion properties than the non-ion-nitrided samples. The higher the nitriding temperatures or the longer the nitriding time, the better the corrosion resistance is. It should also be noted from Fig. 2 that the corrosion resistance of the non-ion-nitrided $Ti_{50}Ni_{50}$ alloy is better than that of the non-ion-nitrided $Ti_{50}Ni_{40}Cu_{10}$ alloy. However, ion-nitrided $Ti_{50}Ni_{50}$ and $Ti_{50}Ni_{40}Cu_{10}$ alloys have almost the same corrosion resistance.

Surface morphologies after the immersion tests for equiatomic TiNi specimens without and with ion nitriding are shown in Figs. 3 and 4, respectively. Those for $Ti_{50}Ni_{40}Cu_{10}$ specimens are similar to Figs. 3 and 4 and therefore are omitted here. Fig. 3(a and b) show the surface morphologies of non-ion-nitrided specimens after immersion in a 1 M HCl solution for 14 days and in a 1 M H_2SO_4 solution for 5 days, respectively. Fig. 4(a) shows the surface morphology of a specimen ion nitrided at condition 3 of Table 1 and then immersed in a 1 M HCl solution for 14 days. Fig. 4(b) shows the surface morphology of a specimen ion nitrided at condition 6 of Table 1 and then immersed in a 1 M H_2SO_4 solution for 5 days. The weight loss corresponding to the specimens of Figs. 3 and 4 has been listed in Fig. 2.

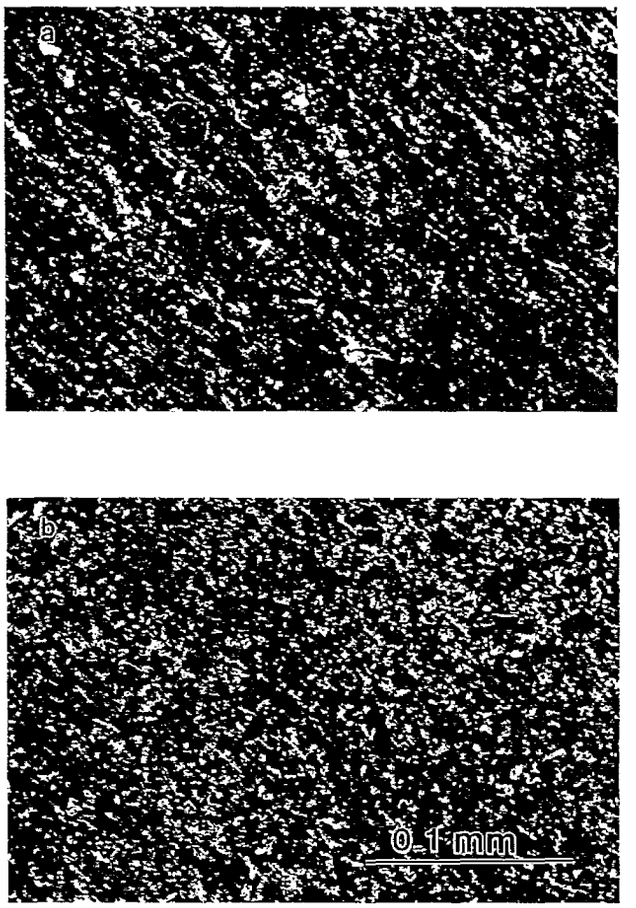

Fig. 3. Scanning electron micrographs of the surface morphology of non-ion-nitrided equiatomic TiNi alloys after immersion in: (a) 1 M HCl solution for 14 days; (b) in 1 M H_2SO_4 solution for 5 days.

From these experimental results shown in Figs. 2–4, one can see that the non-ion-nitrided specimens are easily attacked by 1 M HCl and H_2SO_4 solutions. However, their corrosion properties in both 1 M HCl and H_2SO_4 solutions can be markedly improved by ion nitriding even at low nitriding temperatures and short nitriding times, as indicated from the low weight loss in Fig. 2 and slightly attacked surface morphologies in Fig. 4. Meanwhile, the improvement in corrosion resistance in 1 M HCl solution after ion nitriding is found to be more evident than in 1 M H_2SO_4 solution.

3.2. Electrochemical potentiodynamic behavior

Typical potentiodynamic scanning diagrams for equiatomic TiNi specimens treated in a 0.5 M HCl solution are shown in Fig. 5: (a) without and (b) with ion nitriding at 700 °C for 2 h. The anodic potentiodynamic polarization curve of Fig. 5 is shown in Fig. 6. Values of the corrosion potential ϕ_{corr} and the corrosion current density i_{corr} from Tafel extrapolation are listed in Table 2. The data for ϕ_{corr} and i_{corr} for $Ti_{50}Ni_{40}Cu_{10}$ alloy are also listed in Table 2. From Table 2, one can see that

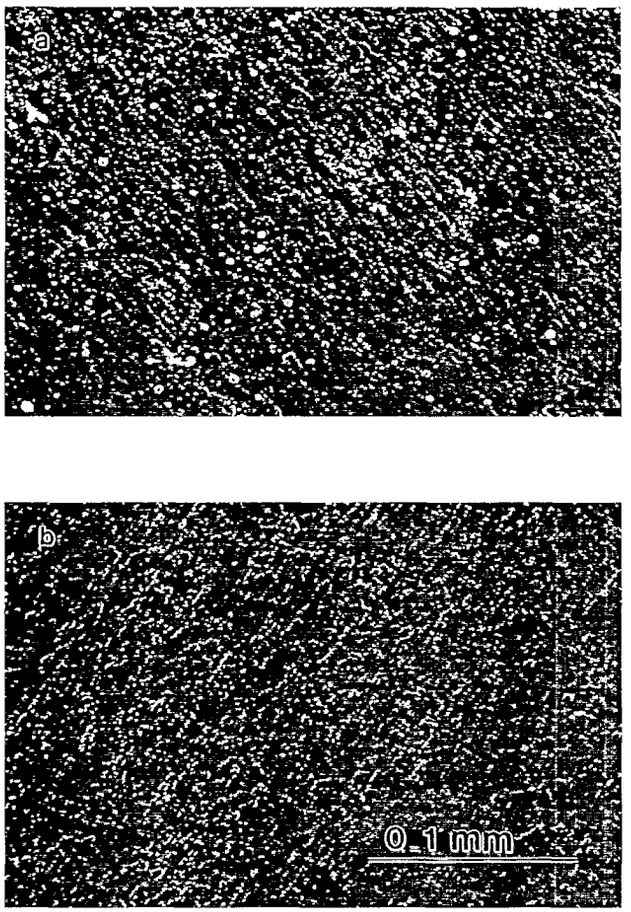

Fig. 4. Scanning electron micrographs of the surface morphology of ion-nitrided equiatomic TiNi alloys after immersion in: (a) 1 M HCl solution for 14 days; (b) in 1 M H_2SO_4 solution for 5 days.

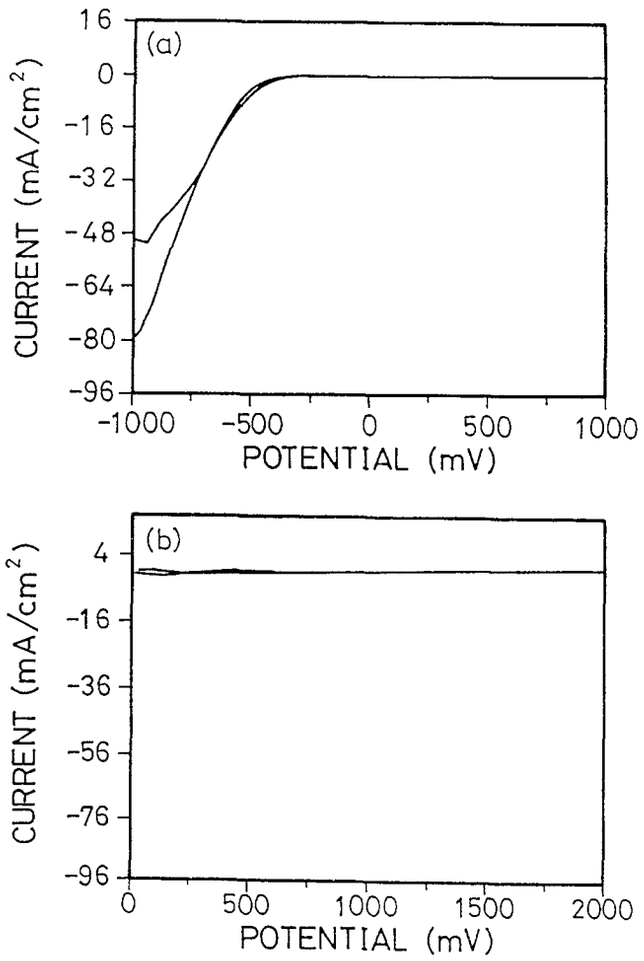

Fig. 5. Potentiodynamic scan diagrams for equiatomic TiNi specimens treated in 0.5 M HCl solution: (a) non-ion-nitrided specimen; (b) ion-nitrided specimen.

the corrosion potential ϕ_{corr} of ion-nitrided $Ti_{50}Ni_{50}$ and $Ti_{50}Ni_{40}Cu_{10}$ specimens is higher, but the current density i_{corr} is lower, than the corresponding values for non-ion-nitrided specimens. This means that the ion-nitrided specimens will exhibit better corrosion properties in the acid solutions.

3.3. A discussion on the effect of ion nitriding on the corrosion properties of TiNi alloys

As mentioned in Part I of this study, the ion-nitrided TiNi specimens consist of the TiN and Ti_2Ni phases in the compound layers [10]. At the same time, higher nitriding temperatures and longer nitriding times cause thicker nitrided layers. It has been reported that TiN is more chemically inert and electrically insulating than titanium alloys [11]. Although the Ti_2Ni phase was reported to have a poor corrosion resistance [18], we believe that TiN phase existing in the outermost part of the compound layers makes ion-nitrided TiNi alloys more chemically inert than non-ion-nitrided TiNi alloys. This suggestion is also supported by the results of Fig. 2 and Table 2, in which the weight loss and corrosion current density of ion-nitrided TiNi specimens show lower values and the corrosion potential shows a higher value than those of non-ion-nitrided specimens. This is because TiN layer provides better corrosion resistance than non-ion-nitrided TiNi alloys in the acid solutions.

3.4. Wear characteristics of ion-nitrided TiNi alloys

Fig. 7 shows the surface morphologies of worn tracks after sliding wear for the equiatomic TiNi specimens without and with ion nitriding (a and b, respectively). Those for $Ti_{50}Ni_{40}Cu_{10}$ specimens are similar to Fig. 7(a and b) and therefore are omitted here. In Fig. 7(a), a typical worn morphology of TiNi martensite is observed. The TiNi martensite (Hv = 200) is so much softer than the against-wear SKS-95 steel (Hv = 700); hence, the adhesive and abrasive wears occur. The adhesive wear will cause fragments of TiNi martensite to be pulled off and to adhere to the surface of the against-wear SKS-95 steel. The abrasive wear introduces ploughing grooves, which originate from the interaction of micro-

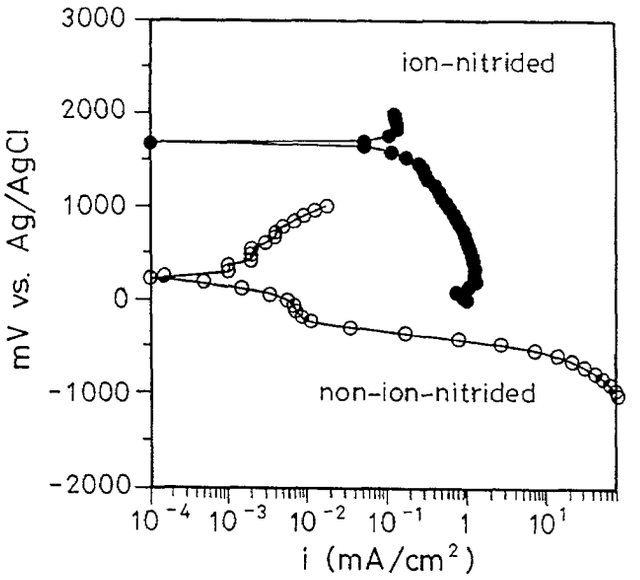

Fig. 6. Anodic potentiodynamic polarization curves for the ion-nitrided and non-ion-nitrided equiatomic TiNi specimens in 0.5 M HCl solution.

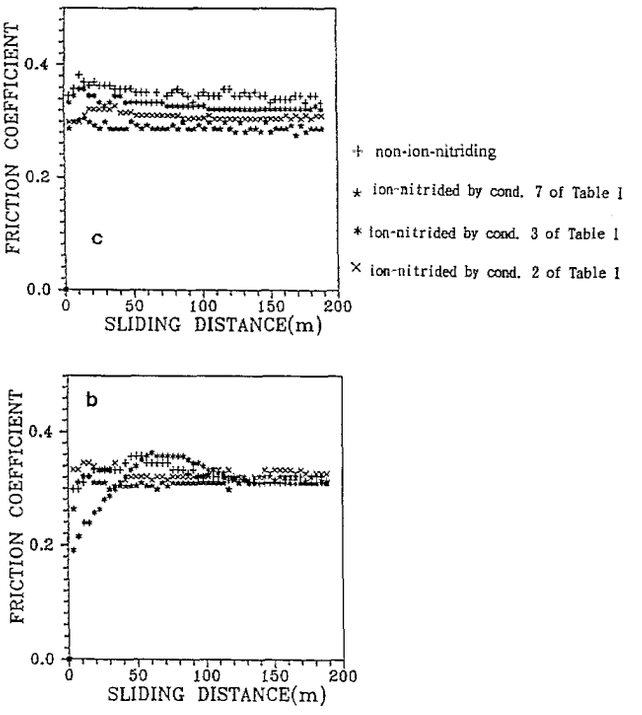

Fig. 8. The friction coefficients for the ion-nitrided TiNi specimens at various nitriding conditions: (a) $Ti_{50}Ni_{50}$; (b) $Ti_{50}Ni_{40}Cu_{10}$ alloys.

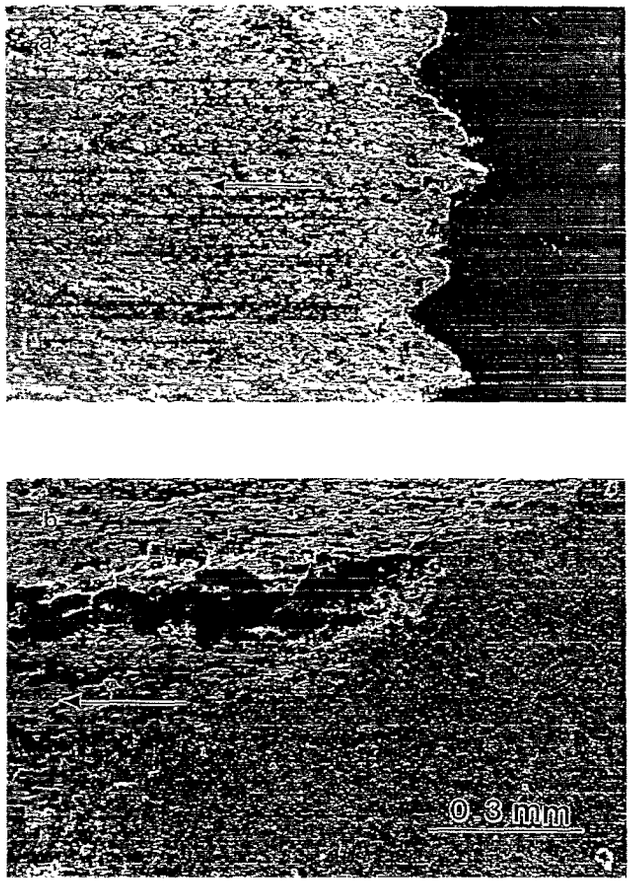

Fig. 7. Surface morphologies of worn tracks after sliding wear for: (a) non-ion-nitrided; (b) ion-nitrided equiatomic TiNi specimens.

cutting and plastic deformation [19]. As presented in Part I of this study, the surface hardness of TiNi martensite can be rapidly raised by ion nitriding. This feature originates from the hard layers of TiN and Ti_2Ni compounds. The thicker the compound layers, the higher the surface hardness. These hard compound layers will affect the wear resistance of TiNi specimens. As shown in Fig. 7(b), main adhesive wear morphology occurs; however, now, fragments of SKS-95 steel have been adhesively transferred to the TiN/Ti_2Ni compound layers, instead of the TiNi martensite being transferred to the steel, due to their significant difference of hardness.

Figs. 8 and 9 shows friction coefficients and wear rates, respectively, for the ion-nitrided $Ti_{50}Ni_{50}$ and $Ti_{50}Ni_{40}Cu_{10}$ specimens at various nitriding conditions of Table 1. In these figures, friction coefficients and wear rates of ion-nitrided specimens are much lower than those of non-ion-nitrided specimens. These results come from the fact that the wear interfaces are TiN/Ti_2Ni compound layers and SKS-95 steel, and hence friction coefficients and wear rates maintain low values due to their high hardness. This indicates that the wear characteristics of TiNi specimens can be effectively improved by ion nitriding because TiN/Ti_2Ni compound layers provide an important contribution to the improvement of wear resistance. In other words, the ion-nitrided TiNi shape memory alloys, being hardened by TiN/Ti_2Ni compounds, can exhibit excellent wear resistance and a low friction coefficient.

Table 2
Corrosion data of the Tafel slope extrapolation calculated from Fig. 6 (0.5 M HCl solution)

Sample	Corrosion potential ϕ_{corr} (V versus Ag/AgCl)	Corrosion current density i_{corr} (mA cm^{-2})
$Ti_{50}Ni_{50}$ (non ion-nitrided)	+0.22	0.0018
$Ti_{50}Ni_{40}Cu_{10}$ (non ion-nitrided)	+0.07	0.0400
$Ti_{50}Ni_{50}$ (ion-nitrided)[a]	+1.68	0.0011
$Ti_{50}Ni_{40}Cu_{10}$ (ion-nitrided)[a]	+1.70	0.0010

[a]ion nitrided at 700 °C for 2 h and 6 torr with $[N_2]/[H_2]=10$.

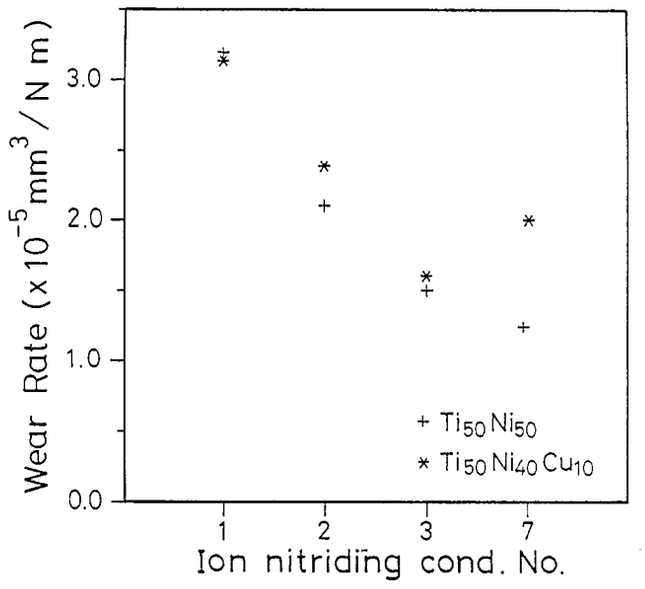

Fig. 9. The wear rates for the ion-nitrided $Ti_{50}Ni_{50}$ and $Ti_{50}Ni_{40}Cu_{10}$ specimens at various nitriding conditions. The ion-nitriding conditions are listed in Table 1.

4. Conclusions

In this study, the corrosion properties and wear characteristics of equiatomic TiNi shape memory alloys with and without ion nitriding were investigated. The experimental results indicate that the non-ion-nitrided specimens are easily attacked by HCl and H_2SO_4 solutions. The corrosion rate of TiNi alloys in both HCl and H_2SO_4 solutions can be markedly improved by ion nitriding. The improvement in corrosion resistance in HCl solution is more evident than that in H_2SO_4 solution. The improved corrosion resistance in these solutions is attributed to the TiN compound formed on the outermost part of the ion-nitrided layers. The wear characteristics of $Ti_{50}Ni_{50}$ and $Ti_{50}Ni_{40}Cu_{10}$ shape memory alloys can also be effectively improved by ion nitriding. The ion-nitrided TiNi specimens, being hardened by TiN/Ti_2Ni compounds, can exhibit an excellent wear resistance and a low friction coefficient.

Acknowledgement

The authors are pleased to acknowledge the financial support of this research by the National Science Council (NSC), Republic of China under Grant No. NSC84-2216-E002-027.

References

[1] S. Miyazaki, K. Otsuka, Y. Suzuki, Scripta Metall. 15 (1981) 287–292.
[2] S. Miyazaki, Y. Ohmi, K. Otsuka, Y. Suzuki, ICOMAT-82, J. Phys. 43 (1982) 255–260.
[3] S. Miyazaki, T. Imai, Y. Igo, K. Otsuka, Metall. Trans. A 17A (1986) 115–120.
[4] Y. Oshia, S. Miyazaki, Corros. Engng 40 (1991) 1009–1025.
[5] K.N. Melton, J.D. Harrison, Proc. International Conference on Shape Memory and Superelastic Technologies, SMST-94, 1994, pp. 187–196.
[6] K. Endo, R. Sachdeva, Y. Araki, Ohno, Proc. International Conference on Shape Memory and Superelastic Technologies, SMST-94, 1994, pp. 197–201.
[7] S. Lombardi, L.H. Yahia, J.E. Klemberg-Sapieha, D.L. Piron, A. Selman, C.H. Rivard, G. Drouin, Proc. International Conference on Shape Memory and Superelastic Technologies, SMST-94, 1994, pp. 221–226.
[8] G. Rondelli, B. Vicentini, A. Cigada, Corros. Sci. 30 (1990) 805.
[9] American Society for Metals, ASM Handbook, vol. 4, 9th ed., ASM, Metals Park, OH, 1991, p. 387.
[10] S.K. Wu, C.L. Chu, H.C. Lin, Surf. Coatings Technol. 92 (1997) 197–205.
[11] J. Aromma, H. Ronkainen, A. Mahiout, S.-P. Hannula, Surf. Coatings Technol. 49 (1991) 353.
[12] M. Taguchi, J. Kurihara, Mater. Trans. Jap. Inst. Metals 33 (7) (1992) 691.
[13] Y. Massiani, P. Gravier, J.P. Crousier, L. Fedrizzi, M. Dapor, V. Micheli, L. Roux, Surf. Coatings Technol 52 (1992) 159.
[14] I.M. Penttinen, A.S. Korhonen, E. Harju, M.A. Turkia, O. Forsen, E.O. Ristolainen, Surf. Coatings Technol. 50 (1992) 161.
[15] F.D. Lai, T.I. Wu, J.K. Wu, Surf. Coatings Technol. 58 (1993) 79.
[16] A. Takasaki, K. Ojima, Y. Taneda, Scr. Metall. 30 (9) (1994) 1095–1098.
[17] C.L. Chu, S.K. Wu, Surf. Coatings Technol. 78 (1996) 219–226.
[18] R.S. Ruta, Corrosion 28 (3) (1993) 217–221.
[19] O. Vingsbo, Wear of Materials, ASME, New York, 1979, pp. 620–635.